TOWARD SHINGLING INTERCONNECTION WITH SHJ SOLAR CELLS

C. Carrière[1]*, V. Barth[1], A. Bettinelli[1], S. Harrison[1], A. Derrier[1], L. Cerasti[2], M. Galiazzo[2]
[1]CEA-LITEN, INES, 50 avenue du Lac Léman, F-73375 Le Bourget-du-Lac, France
[2]Applied Materials Italia Srl, Via Postumia Ovest 244, Olmi di San Biagio di Callalta (TV) Italy
*Corresponding author: vincent.barth@cea.fr

ABSTRACT: Increasingly commercialized, the shingle interconnection technology is known today as a reliable method to interconnect solar cells, and which offers several advantages, such as area performance increase, aesthetic improvement, etc. Silicon heterojunction (SHJ) solar cells that allow high energy conversions (>25 %) [1-2] and a high bifaciality ratio have been integrated in this study project. In the framework of the European HighLite project, the purpose of this research is to bring the shingle technology with SHJ solar cell to a higher technological maturity level (TRL 6-7). In this paper, we present the performances and a preliminary reliability assessment of the first shingle modules, manufactured with SHJ solar cells in an industrial environment, with strings manufactured on a newly developed state-of-the-art industrial stringer.
Keywords: SHJ solar cells, shingle interconnection, reliability, thin wafer.

1 INTRODUCTION

Shingle interconnection technology is one of the alternative interconnection techniques that have emerged in the photovoltaic market over the last 15 years. Long overlooked since its invention in 1960, the rise of high-efficiency and highly bifacial solar cell technologies has brought shingle technology back to the forefront. In particular thanks to its multiple advantages, such as: the elimination of the space between the cells increasing the active surface per module; the absence of busbars; a reduction of resistive losses and a highly aesthetic appearance due to the absence of ribbons and busbars visible on other types of modules.

Increasing number of module manufacturers are now offering a shingle product on the market (Seraphim, SunPower, Solaria, etc.) and according to the ITRPV forecast [3], this technology might gain a market share of more than 10 % in the next decade, together with the paving/overlapping technology. All shingle modules available on the market are currently based on standard cell technology (Al-BSF or PERC). Today, this technology is still under intensive research to determine the best combination of layout, materials and techniques to reduce optical and resistive losses and therefore increase the performance of shingle solar modules.

Heterojunction solar cells presents high efficiencies (>25%), a low temperature coefficient (-0.23%/°C to 0.3%/°C) [4] and a high bifaciality ratio of more than 91 %. SHJ technology is expected to increase market share within the coming years and several companies are currently investing in this technology (Panasonic, REC, EGP, etc.) [5]. Combining shingling and SHJ cells could be a promising way to further increase performances and competitiveness of the solar industry.

However, as SHJ solar cells are highly sensitive to surface and edge defects introduced by cutting process, but also to high temperatures, higher than 200°C, several key challenges must be addressed and certain precautions must be taken upstream to avoid degradation of cell performance during the shingling assembly.

In this work, we present the preliminary results obtained in the framework of the HighLite project, on the first SHJ shingle modules we manufactured at CEA, with solar cells produced within a full industrial environment and assembled in strings via an industrial dedicated shingling stringer.

2 PROJECT RATIONALE

The H2020 European HighLite project focuses on bringing to a high technology readiness level (TRL 6-7) two competing technologies. On one side the Shingle assembly of SHJ solar cells, and on the other side the Back-contact assembly of Interdigitated back-contact (IBC) solar cells. The high performance modules developed throughout the project will demonstrate lower costs and improved environmental profiles compared to current PV modules available in the today market.

In this framework, CEA-INES is in charge of developing the Shingle assembly with SHJ solar cells. Heterojunctions cells manufactured at CEA pilot-line must demonstrate high-efficiencies; basically more than 23.5 % on full-size cells and more than 23.3 % on singulated cells or cut-cells. The implementation of methods to reduce cut-edge recombination in the SHJ fabrication process must be addressed. In this scope, high-efficiency SHJ modules fabrication, with higher yield than 22 % for BAPV, than 21 % for BIPV, may be achievable.

3 EXPERIMENTAL SET-UP

The study carried out at CEA-INES aims to determine the best possible combination(s) of integration and manufacturing parameters in order to produce high-performance and highly reliable SHJ shingle modules.

In the next paragraphs, we present the fabrication steps of SHJ shingle cells and modules.

3.1 Solar cell fabrication

Different splits of SHJ solar cells have been manufactured within the CEA-INES pilot-line. Two main large splits were produced, one with SHJ solar cells of 160 µm thickness and one with 120 µm thick cells.

Focusing on the 160 µm thick solar cells, two metallization-step parameters were varied in order to assess and compare the electrical output performances. These metallization parameters were: i) the printing configuration: single-printed and double-printed process of the metallic grid, on the front-side of the solar cell and ii) the finger density on the back-side (BS) of the cell. Concerning only the rear-side metallization: the pitch, or distance between the fingers, was set at 0.7 mm for one

group of cells and at 0.35 mm for another group.

On the other hand, the split of cells with 120 µm thickness was divided in two parts. Both parts were printed with two different serigraphy screens. The two screens differ in their mesh configuration: one can print 212 pads on the busbar level while the other can print 420 pads. These pads have been designed to allow the contact between the Electrically Conductive Adhesive (ECA) layer, the silver metallisation and the ITO on the cell surface, hence forming the mechanical and electrical bonds linking two adjacent cut-cells.

3.2 Module manufacturing

Once the SHJ solar cells have been printed with low-temperature silver paste on both front and back-side, the solar cells are introduced in an industrial state-of-the-art shingle stringer, developed by Applied-Materials, to be assembled into shingle strings. The first step of the stringing process is to apply onto the surface of the cell a laser grooved trench to delineate the future cleavage of solar cell stripes. In our case, for a typical low-temperature Ag paste, a cut-cell of 26.13 mm (representing 1/6 of a full-size cell) was found to be the optimum stripe width, with little impact from the cut losses and from the line resistance (e.g. Fig. 1).

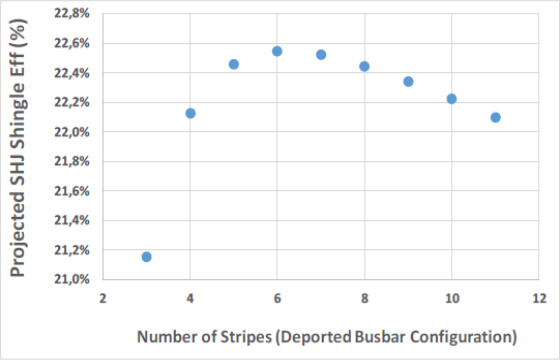

Figure 1: Calculated impact on efficiency of the number of SHJ shingle stripes considered for a given mother cell and usual low-temperature paste resistivity.

Solar cells are then screen-printed with a desired quantity of ECA paste according to an upstream designed pattern. Thereafter the cells are divided into 6 stripes after the cleavage process and are assembled into shingling configuration, with an overlap of 1 mm. Cut-cell stripes from the cell edges are separated from those in the center and are assembled in shingle together apart, forming a pseudo-square (PSQ) string. Once the shingling assembly is finished, an output ribbon is glued on both string ends before passing through an oven for the ECA curing step.

To avoid introducing unsought influencing factors, test-modules manufacturing process was kept identical for all the produced strings. Only one BOM, certified by CEA-INES, was used for the manufacturing process, with the following configuration: glass-glass architecture and thermoplastic polyolefin as encapsulant (e.g. Fig. 2).

All test-modules underwent electrical (I-V) characterization, under STC conditions, by means of a Spire I-V flash tester (230ms Single Long Pulse Xenon Flasher) from Eternal Sun. Electroluminescence (EL) images were obtained with the LumiSolar Professional system from Greateye.

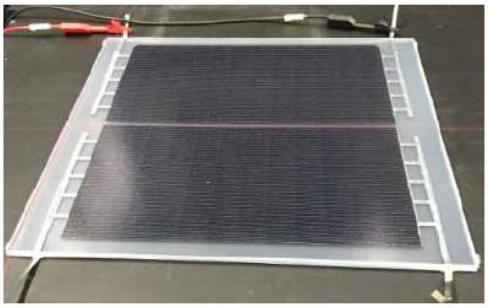

Figure 2: Test-module manufactured at CEA-INES, consisting in two independent strings of 12 cell stripes in series.

4 RESULTS & DISCUSSION

Large volume of SHJ cells, with M2 commercial wafers used, were produced in full automation mode, on the CEA-INES production pilot line [1]. Highly promising efficiencies were reached at full cell level for the very first SHJ shingle cells batch, despite a limited metallization optimization, reaching up to 22.32 % in average for double printed cells (DP) and 22.26 % for single printed cells (SP). Best solar cells were selected and dedicated to the strings fabrication with an average efficiency of 22.40 % for DP cells and of 22.35 % for SP cells.

Two independent strings of 12 cut-cells in series were put together into test-modules (minimodules) as an equivalent 2-cells string. A total of 39 minimodules, or 78 independent strings, were produced and underwent electrical characterization (I-V measurements and EL) in the premises of CEA-INES.

4.1 Electrical characteristics

The average value of power output and FF measured for the entire group of minimodules reached up to 10.12 W and 78.5 % respectively, in STC conditions. To give an insight, minimodules fabricated with the same BOM and with SHJ solar cells adapted to the Smartwire technology (SWCT) configuration and assembled in two independent SWCT 2-cells strings, reached an average power output and FF of 10.03 W and 80.03 % respectively.

The CTM ratio calculated here is the efficiency-based CTM(η), which describes the ratio between the efficiency of the string (taking into account its active surface) and the efficiency of the solar cells that form the string before integration and/or interconnection (e.g. Eq. 1). In our case, solar cells being sorted by efficiency class, the used cells efficiency in the calculation is the measured efficiency for a full-size cell, prior to any cutting process.

$$CTM\ (\eta) = \frac{\eta string}{\eta cell} \times 100 \qquad (1)$$

The average CTM(η) ratio calculated for all the 39 shingle test-modules reached up to 95.6 %. This is an excellent result knowing that this CTM(η) value takes into account the losses due to the cutting process [6].

4.2 Impact of the cell thickness

The plotting of the power output values and the CTM ratios of all the strings made with standard thickness cells (160 µm) versus thinner cells, at 120 µm, is depicted in the Figure 3. Average Pmax of thinner-cells based strings shows a higher value of 1.83 % compared to the one of the 160 microns cells. CTM ratios follows the same pattern with

a difference between the two thicknesses of 1.55 % (e.g. Fig. 3). In general, as 160 µm and 120 µm cells electrical characteristics are considered equivalent, the explanation behind the higher performances reached by the thinner-cells strings is certainly linked to the metallization process step during the solar cell manufacturing. The quantity of silver paste printed onto the cell surface is slightly larger for the thinner cells. The surface texturization, being different from the 160 microns cells, the wetting of the silver paste deposited will differ depending on the shape characteristics of the pyramids and the ITO layer homogeneity. In the case of the thinner cells, pyramids on the surface have a larger base than for the standard cells, thus the paste is less evenly spread during deposition, making fingers slightly larger. Also during the metallization process, screen-printing parameters vary on a small scale from one thickness to another, which may lead to a finger height and/or width to be increased. However, such results are promising and proves that shingle assembly technology is compatible with thin solar cells technology.

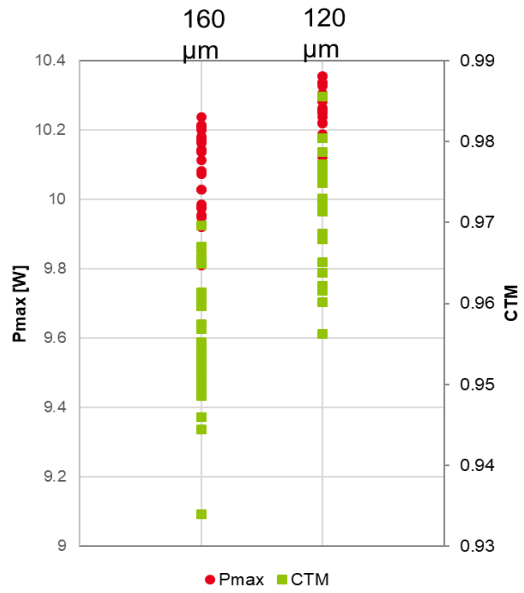

Figure 3: Pmax and CTM ratio plots of standard SHJ cells (160 µm) based shingle strings vs thinner-wafer cells (120 µm).

4.3 Metallization parameters variation results

To assess the impact of the metallization configuration, initial electrical responses of the selected test-modules were measured. For the first studied parameter: the printing configuration, average module performances are very promising with a STC power output of 9.92 W for SP cells and of 10.07 W for DP cells (see Table I). Double-printing the metallic grid increases the finger aspect ratio, hence reduces the line resistance. As expected, a higher FF is obtained with the DP cells. Over 21.0 % of average string efficiency was calculated for both SP and DP configurations. The average CTM ratio calculated for DP cells is 1 % higher than the one of SP cells. The reliability and the resilience of the metallic grids to the thermomechanical stress applied on these two configuration will be assessed when aging tests results are available.

Table I: Electrical performances of the first SHJ minimodules produced on the CEA-INES platform in shingle configuration.

Solar cells	Voc (V)	Isc (A)	Pmax (W)	Vmax (V)	Imax (A)	FF
SP	8.775	1.469	9.917	7.247	1.369	0.769
DP	8.778	1.465	10.070	7.311	1.377	0.783

Regarding the impact of the finger density on the rear side of the cells, we compared performances of both kind of cells BS grid. The average power output measured for more-dense metallization based strings with a pitch of 0.35 mm is very similar to the average Pmax of the less-dense BS cells, albeit lightly higher of about 0.3 %. Same observation can be done for the CTM ratio comparison of each configuration (e.g. Fig. 4). The obtained results finally show that the BS finger density has very little impact on the initial performances; although accelerated aging tests results might reveal further differences.

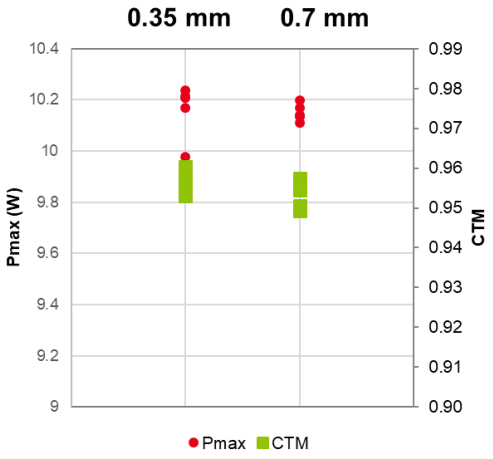

Figure 4: Power output and CTM ratio plots of back-side 0.35 mm vs 0.7 mm pitch cells configurations.

4.4 Electrically conductive adhesive quantities

Since the ECA-based gluing process - ensuring the electrical and mechanical contact between the cells - is the core of the shingling interconnection concept, we focused on this parameter to assess the electrical and mechanical behavior of these strings.

As described in the module manufacturing process paragraph, two serigraphy screens at the metallization process level were used on specific solar cells. All the solar cells tested in this experiment have a thickness of 120 µm. The purpose of the test is to observe first the initial electrical characteristics and second the reliability of the strings after thermal cycling tests. On the solar cells designed with 420 metallic pads, two different quantities of ECA paste have been deposited in the printer block of the shingle stringer. On one group of cells we deposited a standard quantity of 20 mg in total (on the whole full-size cell, prior to the cutting process), and on the other group the double quantity was deposited: 39 mg. Concerning the solar cells with the 212 metallic pads configuration, the standard ECA consumption was divided by 2, hence 10 mg of paste deposited in total onto the solar cells.

Initial performance results are depicted in Figure 5. Focusing on the printed 420 pads cells, the difference in average Pmax and average CTM ratio between cells with 20 mg and 39 mg is minor, around 0.6 % higher for the

20 mg cells. It means that using a lower quantity of ECA gives higher performances (e.g. Fig. 5).

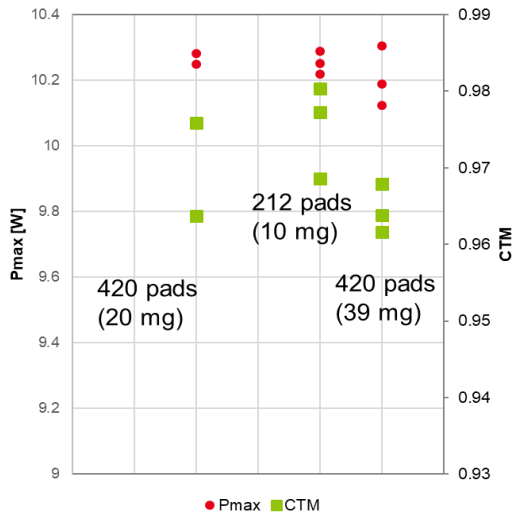

Figure 5: Power output and CTM ratio plots of different ECA quantities and metallic pad configurations.

One explanation related to the ECA application could be given. Metallic pads are designed to receive a certain amount of ECA paste. When this amount is doubled, the added quantity may outpace the pads frame and be more easily spread out, potentially causing local stress after the curing step or reaching solar cell edge when the adjacent cell is overlapped, causing local shunt areas.
Regarding the printed 212 pads cells, and the very limited ECA quantity (10 mg), average Pmax and CTM values are very close to the ones of the 420 pads with 20 mg of ECA.

Hence, at the initial performances level, we may consider that a double quantity of ECA paste is not bringing any improvement in the electrical characteristics, rather, it could be more beneficial to deposit lower quantities. Nevertheless we expect different behaviors of these cells under thermal cycles stress.

4.5 Accelerated aging tests results

Thermal cycling tests are the current type of accelerated aging tests we apply to our minimodules, as the purpose is to monitor and observe the behavior of the shingle interconnections, at the overlaps levels and at the ribbons gluing attachment level; after repeated thermomechanical solicitations.

Results presented in this section relate to the group of test-modules that underwent 500 thermal cycles. This group is the one used for the performances study of single print and double print configuration. Initially, these test-modules have been manufactured, laminated and characterized afterward at CEA-INES. Systematic electroluminescence images have shown no lamination-induced degradation, such as breakage or cracks occurrence nor propagation of existing ones.

Thermal cycling tests are currently ongoing and the objective is to reach 800 or 1000 cycles for all the test-modules.

The following EL images depicts the evolution of a string aging from post-lamination to TC 500 (e.g. Fig. 6). So far, up to now, no particular change has been visually detected, no cracks or shunt areas occurred during the thermal stress processing.

Vertical darker lines visible on each cell in the EL images correspond to the full-size cell manufacturing process at the pilot-line level and are not related to the current reliability study.

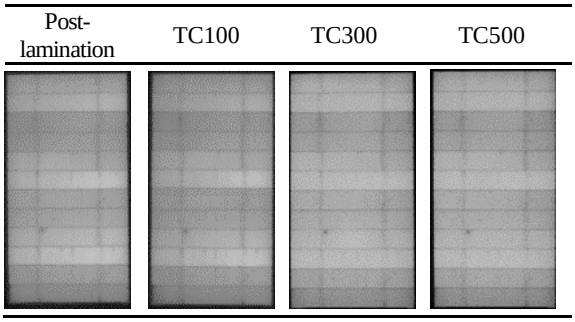

Figure 6: EL images of one 12-cells shingle string after the lamination process, after 100, 300 and 500 thermal cycles.

Minimodules that underwent 500 thermal cycles and are still being tested. Results after 500 cycles are very promising and encouraging since all the tested strings show very little losses in power output and FF (e.g. Fig. 7). The range of the degradation so far is between 0.5 and 1 % of power losses.

Nevertheless, at TC 500, the average Pmax degradation for SP cells is of 1.44 % and of 1.04 % for the DP cells, therefore a relative difference of 27.7 % between the two configurations. Further results will provide extra information on the SP and DP cells resilience to the accelerated aging tests.

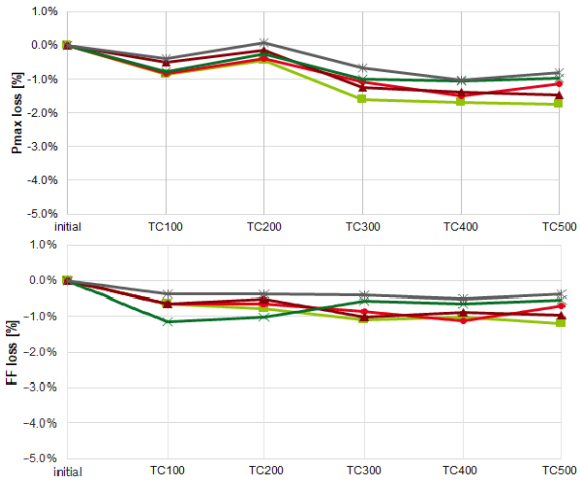

Figure 7: Power and FF losses evolution of the minimodules from the initial state to after 500 thermal cycles.

5 SCALING-UP APPROACH

As a step forward in this study, the fabrication of longer shingle strings was achieved with a string configuration of 37 cells in series, instead of 12 as for the minimodules manufacturing campaigns.

These longer strings were also manufactured with different thicknesses solar cells: 160 µm and 120 µm.

A part of the long strings (of both thicknesses) was integrated independently into large modules, still with the same certified BOM used for the test-modules. Here again,

the aim is to monitor the longer strings interconnections behavior under thermal stress.

Under same module manufacturing conditions, five strings (of 160µ solar cells) were bussed in parallel successfully, thus forming a 60-cells equivalent half-module. Initial electrical performances were measured after the lamination process. Post-lamination EL imaging of the half-module shows no breakage or crack defects (Fig. 8).

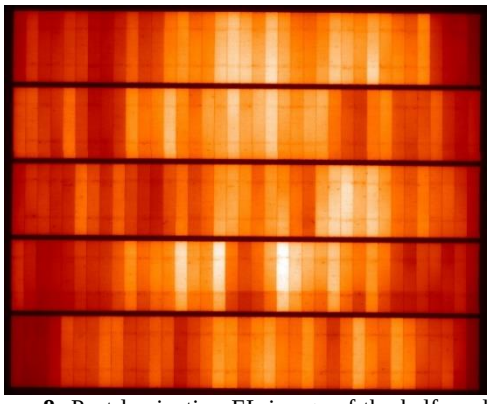

Figure 8: Post-lamination EL image of the half-module, with 5 strings of 37 cell in series each bussed in parallel.

Results of initial electrical measurements are promising and very encouraging (see Table II). Here also, performances of the strings made of thinner-cells are higher than the 160 microns cells-based strings. The relative differences of the average Pmax and CTM values of both 120 and 160 µm cells need to be further assessed to thoroughly understand and identify the main factors that could act on performances slight decrease in general.

Table II: Electrical performances of the SHJ shingle half-module and long independent shingle strings.

	Thick (µm)	Voc (V)	Isc (A)	Pmax (W)	FF	CTM %
Half-module	160	26.95	7.16	149.36	0.77	92.9
Average strings		27.0	1.43	29.96	0.78	93.6
Average strings	120	27.26	1.42	30.45	0.79	94.5

6 CONCLUSION AND PERSPECTIVES

In this paper, we presented an overview of the early development and implementation stages of the SHJ shingle technology in the framework of the European HighLite project. SHJ solar cells manufactured at CEA-INES were designed, namely at the metallization process step, to be further assembled into shingle configuration with the help of a state-of-the-art shingle stringer, developed by Applied-Materials. Test-modules manufactured at the CEA premises, using shingle strings of 12 cells in series each and using a particular BOM certified by CEA, have given highly promising initial electrical results.

Part of them were aged in climatic chamber to reach 500 thermal cycles. Preliminary reliability results were very encouraging since overall power losses after TC 500 did not exceed 1 % for the tested group of minimodules.

Technical experiments linked to the metallization patterns and the ideal ECA paste quantity to deposit have shown that:

- High power output can be reached by thinner cells, of thickness 120 µm.
- Metallization double-printed DP configuration is preferable but the relative difference between SP and DP cells powers is minor, of about 1.5 %.
- DP cells present for the moment a slight higher resilience to thermal cycling tests.
- The rear-side finger density has very little impact on the initial performances.
- Lower quantities of ECA paste deposited on the cells give higher absolute performances but have finally low impact on the initial electrical characteristics.
- Low quantities of paste deposition process are compatible with thinner-cells, giving high power output.

Further reliability study will allow to see the evolution of the performances depending of the tested parameters, as well as the resilience of the ECA paste based interconnections, at the overlap and ribbons level.

We also achieved a successful integration of first SHJ long strings: either in isolated configuration or in parallel (5 strings: Half-module). Performances of these large modules are promising and a reliability study will be conducted when further results of thermal cycling tests are available.

The perspectives of this work are mainly the manufacturing of an advanced 72 cells equivalent shingle module with SHJ cells and the follow-up of the interconnections reliability studies currently ongoing, with indoor and outdoor aging monitoring.

ACKNOWLEDGMENT

The authors would like to gratefully acknowledge the support of the European Union through the funded H2020 project HighLite under Grant Agreement no. 857793.

The authors would also like to thank Stefan Wendlandt of PI-Berlin, partner within the HighLite project, for carrying out part of the accelerated ageing tests' campaign at PI-Berlin premises.

REFERENCES

[1] A. Danel et al, Silicon Heterojunction Cells with Open Circuit Voltage Over 750mV, European Photovoltaic Solar Energy Conference (35th EU PVSEC), 2018.

[2] PV-Magazine article (01/2020): https://www.pv-magazine.com/2019/11/20/hanergy-sets-new-heterojunction-module-efficiency-record/

[3] 11th Edition of the International Technology Roadmap for Photovoltaic (ITRPV 2020).

[4] J. Haschke, et al., "The Impact of Silicon Solar Cell Architecture and Cell Interconnection on Energy Yield in Hot & Sunny Climates", Energy & Environmental Science, (2017).

[5] TaiyangNews Report Heterojunction Solar Technology, 2019.

[6] J. Eymard, et al.,"Performance Simulations of a 72-Cell, a-Si HET Module with Different Tab-Interconnection Geometries", European Photovoltaic Solar Energy Conference (35th EU PVSEC), 2018.